

Ground-state properties of gapped graphene using the random phase approximation

Alireza Qaiumzadeh^{1,2} and Reza Asgari²

¹*Institute for Advanced Studies in Basic Sciences (IASBS), Zanjan, 45195-1159, Iran*

²*School of physics, Institute for research in fundamental sciences, IPM, 19395-5531 Tehran, Iran*

We study the effect of band gap on the ground-state properties of Dirac electrons in a doped graphene within the random phase approximation at zero temperature. Band gap dependence of the exchange, correlation and ground-state energies and the compressibility are calculated. In addition, we show that the conductance in the gapped graphene is smaller than gapless one. We also calculate the band gap dependence of charge compressibility and it decreases with increasing the band gap values.

PACS numbers: 73.63.-b, 72.10.-d, 71.10.-w, 73.50.Fq

I. INTRODUCTION

Graphene is a flat monolayer of carbon atoms tightly packed into a two-dimensional (2D) honeycomb lattice and it is a basic building block for all nanostructured carbon. This stable structure has attracted considerable attention because of experimental progress¹ and because of exotic chiral feature in its electronic properties and promising applications². Very recent experiments on both a suspended graphene and a graphene on substrate have found remarkably high mobility 2×10^5 cm²/Vs for carrier transport³ at room temperature which is two order of magnitude higher than the mobility of silicon wafer used in microprocessors.⁴

An interesting feature of graphene which makes it very applicable in semiconductor technology is the opening a gap in the band energy structure of graphene. There are several scenarios to open a gap in the band energy structure of graphene. One is the finite size effect by using graphene nanoribbons, where gaps give rise to constriction of the electrons in the ribbon and it depends on the detailed structure of ribbon edges.⁵ More precisely, the band gaps with armchair shaped edges originate from quantum confinement and the value of the gap depends on the width of the ribbon. For zigzag shaped edges, on the other hand, the band gaps arise from a staggered sublattice potential due to magnetization at the edges.⁶ Importantly, edge effects plays a crucial role in transport properties. The gap engineering can be also achieved through doping the graphene with chemical species⁷ due to the translational symmetry breaking. The electronic properties of a graphene interacting with CrO₃ molecules has been calculated by using *ab initio* calculations.⁸ This type of calculations, predicts opening a gap about 0.12 eV at the Dirac point. Another scenario is graphene by placing it on top of an appropriate substrate which breaks the graphene sublattice symmetry and, therefore generates an intrinsic Dirac mass for the charge carriers.⁹ Typical substrate is made of hexagonal SiC with a gap about 0.26 eV. A recent band structure calculation for a graphene on top of a hexagonal boron nitride crystal¹⁰ has been shown a band gap about 53 meV. The gap can also be generated dynamically by applying a magnetic field.¹¹ Moreover, when both mono-and bilayer graphene material are covered with water and ammonia molecules, a gap induce in the spectrum of energy.¹² Interestingly, the mechanism that electrons hopping on a honeycomb lattice with textured tight-binding hopping amplitudes, the Kekulé texture, generates a Dirac gap.¹³ Eventually, It has been

suggested that a small gap can be opened on the Dirac points due to spin-orbit coupling or Rashba effect¹⁴ which makes the system a spin Hall insulator with quantized spin Hall conductances.¹⁵

Recently, the local compressibility of graphene has been measured¹⁶ using a scannable single electron transistor. The measured compressibility is claimed to be well described by the kinetic energy contribution and it is also suggested that exchange and correlation effects have canceling contributions. From the theoretical point of view, the compressibility was first calculated by Peres *et al.*¹⁷ considering the exchange contribution to a noninteracting doped or undoped graphene flake. A related quantity $\partial\mu/\partial n$ (where μ is the chemical potential and n is the electron density) is recently considered by Hwang *et al.*¹⁸ within the same approximation and they stated that correlations and disorder effects would introduce only small corrections. This statement is only true in quite large density doped values. To go beyond the exchange contribution, the correlation effects were taken into account by Barlas *et al.*¹⁹ based on an evaluation of graphene's exchange and random phase approximation (RPA) correlation energies. Moreover, Sheehy and Schmalian²⁰ by exploiting the proximity to relativistic electron quantum critical point, derived explicit expressions for the temperature and density dependence of the compressibility properties of graphene. Importantly, the effect of disorder and many-body interactions on the compressibility has been recently studied by us.²¹ We successfully demonstrated the importance of including correlation effects together with disorder effects in the thermodynamic quantities. It should be noticed that all these theoretical efforts have been carried out for a gapless graphene.

Our aim in this work is to study the ground-state properties in the presence of Dirac gap and electron-electron interactions. For this purpose, we derive the gap dependence of the dynamic polarization function for a doped graphene to calculate the scattering rate, ground-state energies and the compressibility of the system at the level of RPA including the opening gap at Dirac point.

We consider different on-site energies for atoms in two sublattices in graphene which is established experimentally to be important when an appropriate substrate such a boron nitride or SiC is used. The compressibility decreases by increasing the band gap values due to the sublattice symmetry breaking.

The rest of this paper is organized as follows. In Sec. II, we introduce the models for dynamic polarization function and ground-state energy calculations. We then outline the calculation of d.c conductivity and compressibility. Section III contains our numerical calculations of ground state properties. We conclude in Sec. IV with a brief summary.

II. THEORETICAL APPROACH

We consider a Dirac-like electron in a continuum model interacting via a Coulomb potential $e^2/\epsilon r$ and its Fourier transform $v_q = 2\pi e^2/(\epsilon q)$ where ϵ is the average background dielectric constant (for instance, $\epsilon \simeq 5.5$ for graphene placed on SiC with the other side being exposed to air) having an isotropic band gap at Dirac points. If one assumes that the sublattice symmetry is broken and α_a , α_b are on-site energies of atoms A and B , respectively, then the contribution of the on-site energies in Hamiltonian of graphene can be written¹¹ as

$$\begin{aligned}
\hat{H}_1 &= \sum_{\mathbf{k},\sigma} [\alpha_a a_\sigma^\dagger(\mathbf{k}) a_\sigma(\mathbf{k}) + \alpha_b b_\sigma^\dagger(\mathbf{k}) b_\sigma(\mathbf{k})] \\
&= \sum_{\mathbf{k},\sigma} \hat{\Psi}_{\mathbf{k},\sigma}^\dagger [\alpha_+ \tau^0 - \alpha_- \tau^3] \otimes \sigma^3 \hat{\Psi}_{\mathbf{k},\sigma}
\end{aligned} \tag{1}$$

where $\alpha_+ = (\alpha_a + \alpha_b)/2$ that corresponds to the same carrier density on two sublattices, $\alpha_- = (\alpha_a - \alpha_b)/2$ is carrier imbalance on two sublattices that leads to break the inversion symmetry and τ^0 is 2×2 unit matrix, τ^3 is a Pauli matrix that acts on K_+ and K_- two-degenerate valleys at which π and π^* bands touch and σ^3 is Pauli matrix that act on graphene's pseudospin degrees of freedom. Consequently, the noninteracting Hamiltonian for a gapped graphene is given by $\hat{H}_0 = \sum_{\mathbf{k},\sigma} \Psi_{\mathbf{k},\sigma}^\dagger \hat{\mathcal{H}}_0 \Psi_{\mathbf{k},\sigma}$ where

$$\hat{\mathcal{H}}_0 = \begin{pmatrix} \Delta & \hbar v \hat{k}^* & 0 & 0 \\ \hbar v \hat{k} & -\Delta & 0 & 0 \\ 0 & 0 & -\Delta & -\hbar v \hat{k}^* \\ 0 & 0 & -\hbar v \hat{k} & \Delta \end{pmatrix} \tag{2}$$

where $\hat{k} = k_x + ik_y$ and σ is the spin of charge carrier. Here, $v = 3ta/2$ is the Fermi velocity, t is the tight-binding hopping integral, a is the spacing of the honeycomb lattice. For the hexagonal crystal structure of graphene, $a = 1.42\text{\AA}$ is the carbon-carbon distance, the tight-bonding hopping energy is $t = 2.8$ eV and the bare Fermi velocity is $v = 10^6$ m/s. In the noninteracting Hamiltonian, \hat{H}_0 the reference energy $(\alpha_a + \alpha_b)\tau_0/2$ is subtracted and the energy gap is defined as $2\Delta = (\alpha_b - \alpha_a)$ where we expect $\Delta < t$. The corresponding four components pseudospinor of the noninteracting Hamiltonian is $\Psi_{\mathbf{k},\sigma}^\dagger = (\psi_{+,\sigma}^b, \psi_{+,\sigma}^a, \psi_{-,\sigma}^a, \psi_{-,\sigma}^b)$. It is easy to diagonalize the noninteracting Hamiltonian based on pseudospinors in the conduction and valance band of energies with eigenvalues given by $\pm\sqrt{\hbar^2 v^2 k^2 + \Delta^2}$. Importantly, the low energy quasiparticle excitations in a gapless graphene are linearly dispersing and it is valid for energy less than 1 eV. Accordingly, the validity of the noninteracting Hamiltonian given by Eq. (2) to explore graphene properties is to the case which $\sqrt{\hbar^2 v^2 k^2 + \Delta^2} < 1\text{eV}$. On the other hand, we shall achieve to a conventional two-dimensional electron gas system by setting $\hbar v k / \Delta \ll 1$.

Finally, the total Hamiltonian including the electron-electron repulsion interaction is given by

$$\hat{H} = \hat{H}_0 + \frac{1}{2S} \sum_{\mathbf{q} \neq 0} v_q (\hat{n}_{\mathbf{q}} \hat{n}_{-\mathbf{q}} - \hat{N}), \tag{3}$$

where S is the sample area and \hat{N} is the total number operator. The presence of a neutralizing background of positive charge is explicit in Eq. (3). As we mentioned in introduction section, this kind of Hamiltonian can be used in graphene by placing it on top of an appropriate substrate that breaks the graphene sublattice symmetry and generates an intrinsic Dirac gap.

A central quantity in the theoretical formulation of the many-body effects in Dirac fermions is the noninteracting dynamical polarizability function^{19,22,23} $\chi^{(0)}(\mathbf{q}, i\Omega, \mu \geq \Delta)$ where μ is chemical potential. Here, we would like to emphasize that we have calculated the gap dependence of the noninteracting polarization function for doped graphene

however the vacuum polarization function in which $\mu = \Delta$ has been calculated by Kotov *et al*²⁴. They studied the distribution of polarization charge induced by a Coulomb impurity for undoped graphene. However, we would like to study the ground-state properties for doped graphene sheets. To achieve this goal, we write the dynamical polarizability function in terms of one-body noninteracting Green's function

$$\chi^{(0)}(\mathbf{q}, \Omega, \mu) = -i \int \frac{d^2\mathbf{k}}{(2\pi)^2} \int \frac{d\omega}{2\pi} \text{Tr}[i\gamma_0 G^{(0)}(\mathbf{k} + \mathbf{q}, \omega + \Omega, \mu) i\gamma_0 G^{(0)}(\mathbf{k}, \omega, \mu)] , \quad (4)$$

where one-body noninteracting Green's function²⁵ by using the noninteracting Hamiltonian is given by

$$G^{(0)}(\mathbf{k}, \omega, \mu) = i \frac{-\gamma_0\omega + \hbar v\boldsymbol{\gamma} \cdot \mathbf{k} + i\Delta}{-\omega^2 + \hbar^2 v^2 k^2 + \Delta^2 - i\eta} - \pi \frac{-\gamma_0\omega + \hbar v\boldsymbol{\gamma} \cdot \mathbf{k} + i\Delta}{\sqrt{\hbar^2 v^2 k^2 + \Delta^2}} \delta(\hbar\omega - \sqrt{\hbar^2 v^2 k^2 + \Delta^2}) \theta(k - k_F) , \quad (5)$$

in which γ -matrices are related to Pauli matrices by $\sigma^3 = -i\gamma_0$ and $\sigma^j = (-1)^j \sigma^3 \gamma_j$ for $j = 1, 2$ and k_F is the Fermi momentum related to the density of electron as given by $k_F = (4\pi n/g)^{1/2}$. $g = g_v g_s = 4$ is valley and spin degeneracy and θ is the Heaviside step function. The chemical potential is given by $\mu = \sqrt{\hbar^2 v^2 k_F^2 + \Delta^2}$ at zero temperature. After implementing $G^{(0)}(\mathbf{k}, \omega, \mu)$ in Eq. (4) and calculating the traces and integrals, the result is given by the follow expression

$$\begin{aligned} \chi^{(0)}(\mathbf{q}, i\omega, \mu) = & -\frac{g}{2\pi v^2} \left\{ \mu - \Delta + \frac{\varepsilon_q^2}{2} \left[\frac{\Delta}{\varepsilon_q^2 + \hbar^2 \omega^2} + \frac{1}{2\sqrt{\varepsilon_q^2 + \hbar^2 \omega^2}} \left(1 - \frac{4\Delta^2}{\varepsilon_q^2 + \hbar^2 \omega^2} \right) \tan^{-1} \left(\frac{\sqrt{\varepsilon_q^2 + \hbar^2 \omega^2}}{2\Delta} \right) \right] \right. \\ & - \frac{\varepsilon_q^2}{4\sqrt{\hbar^2 \omega^2 + \varepsilon_q^2}} \Re e \left[\left(1 - \frac{4\Delta^2}{\varepsilon_q^2 + \hbar^2 \omega^2} \right) \left\{ \sin^{-1} \left(\frac{2\mu + i\hbar\omega}{\varepsilon_q \sqrt{1 + \frac{4\Delta^2}{\varepsilon_q^2 + \hbar^2 \omega^2}}} \right) - \sin^{-1} \left(\frac{2\Delta + i\hbar\omega}{\varepsilon_q \sqrt{1 + \frac{4\Delta^2}{\varepsilon_q^2 + \hbar^2 \omega^2}}} \right) \right\} \right] \\ & - \frac{\varepsilon_q^2}{4\sqrt{\hbar^2 \omega^2 + \varepsilon_q^2}} \Re e \left[\left(\frac{2\mu + i\hbar\omega}{\varepsilon_q} \right) \sqrt{\left(1 + \frac{4\Delta^2}{\varepsilon_q^2 + \hbar^2 \omega^2} \right) - \left(\frac{2\mu + i\hbar\omega}{\varepsilon_q} \right)^2} \right] \\ & \left. + \frac{\varepsilon_q^2}{4\sqrt{\hbar\omega^2 + \varepsilon_q^2}} \Re e \left[\left(\frac{2\Delta + i\hbar\omega}{\varepsilon_q} \right) \sqrt{\left(1 + \frac{4\Delta^2}{\varepsilon_q^2 + \hbar^2 \omega^2} \right) - \left(\frac{2\Delta + i\hbar\omega}{\varepsilon_q} \right)^2} \right] \right\} , \quad (6) \end{aligned}$$

where $\varepsilon_q = \hbar v q$. By setting $\Delta = 0$, it is easy to determine that Eq. (6) reduces to the noninteracting dynamic polarization function of the gapless graphene sheet.¹⁹ Furthermore, for the half-filled gapped graphene sheet, the noninteracting dynamic polarization function, vacuum polarization, is given by²⁴

$$\chi^{(0)}(\mathbf{q}, i\omega, \mu = \Delta) = -g \frac{\varepsilon_q^2}{4v^2\pi} \left[\frac{\Delta}{\varepsilon_q^2 + \hbar^2 \omega^2} + \frac{1}{2\sqrt{\varepsilon_q^2 + \hbar^2 \omega^2}} \left(1 - \frac{4\Delta^2}{\varepsilon_q^2 + \hbar^2 \omega^2} \right) \tan^{-1} \left(\frac{\sqrt{\varepsilon_q^2 + \hbar^2 \omega^2}}{2\Delta} \right) \right] . \quad (7)$$

Using the above results for the noninteracting polarization function on the imaginary frequency axis, the density of state at Fermi energy is calculated as

$$D(\varepsilon_F) = D^0(\varepsilon_F) \left[\left(1 + \Delta^2/\varepsilon_F^2 \right)^{1/2} \right] \theta(\varepsilon_F) , \quad (8)$$

where $D^0(\varepsilon_F) = g\varepsilon_F/2\pi\hbar v^2$ is the density of states of gapless graphene.²² Note that we define $\varepsilon_F = \hbar v k_F$. The linear correction of expanded gapped polarization function for Δ is zero, however the quadratic correction is easily obtained

$$\chi^{(0)}(q, i\omega, \mu) \simeq \chi^{(0)}(q, i\omega, \mu) \Big|_{\Delta=0} - \frac{g}{2\pi v^2} \left[\frac{1}{2} + \frac{\varepsilon_q^2}{\sqrt{\varepsilon_q^2 + \omega^2}} \Re e \left\{ \frac{2 \sin^{-1}(\frac{2\mu}{\varepsilon_q}) - \pi}{\varepsilon_q^2 + \omega^2} - \frac{\sqrt{\varepsilon_q^2 - (2 + i\omega)^2}}{4\varepsilon_q^2} \right\} \right] \Delta^2 + O(\Delta^3), \quad (9)$$

Where the explicit expression of $\chi^{(0)}(q, i\omega, \mu) \Big|_{\Delta=0}$ is given by our group.¹⁹ Now, we are in the stage to use the noninteracting polarization function given by Eq. (6) to calculate some physical quantities.

A. Transport scattering time in a gapped graphene

As a first application of the noninteracting polarization function, we would like to calculate the gapped graphene transport scattering time by randomly distributed impurity centers in the relaxation time approximation.²⁶ The validity of the Born approximation is discussed by Novikov²⁷ and here we use this approximation to calculate qualitatively the graphene transport scattering time. To this purpose, the transport scattering time is given by Boltzmann theory,

$$\frac{1}{\tau(\varepsilon_F)} = \frac{2\pi}{\hbar} \sum_{\mathbf{q}, s, s'} n_i \frac{\langle |v_i(\mathbf{q})|^2 \rangle}{\epsilon(q)^2} (1 - \cos \theta_{\mathbf{q}, \mathbf{q} + \mathbf{k}_F}) F^{s, s'}(\mathbf{q}, \mathbf{q} + \mathbf{k}_F) \delta(s\sqrt{\varepsilon_{\mathbf{k}_F}^2 + \Delta^2} - s'\sqrt{\varepsilon_{\mathbf{q} + \mathbf{k}_F}^2 + \Delta^2}), \quad (10)$$

where $v_i(\mathbf{q}) = \frac{2\pi e^2}{\epsilon q} \exp(-qd)$ is the Coulomb scattering potential between an electron and an out of plane impurity, $\epsilon(q)$ is the static RPA dielectric function appropriate for graphene, $\epsilon(q) = 1 - v_q \chi^{(0)}(q, 0, \mu)$, n_i is the density of impurities and d is the setback distance from the graphene sheet and s, s' being \pm . Since we consider large charge carrier density and elastic scattering, we can therefore neglect interband scattering process. $F^\beta(\mathbf{q}, \mathbf{q} + \mathbf{k}_F)$ is the overlap of states ($\beta = \pm$), which can be easily calculated from the pseudospinors of Hamiltonian, Eq. (2). The result is as follow

$$F^\pm(\mathbf{q}, \mathbf{q} + \mathbf{k}) = \frac{1}{2} \left[1 \pm \frac{1}{\sqrt{\varepsilon_{\mathbf{k} + \mathbf{q}}^2 + \Delta^2}} \left\{ \sqrt{\varepsilon_{\mathbf{k}}^2 + \Delta^2} + \frac{\varepsilon_q \varepsilon_k \cos \phi}{\sqrt{\varepsilon_{\mathbf{k}}^2 + \Delta^2}} \right\} \right], \quad (11)$$

where ϕ is an angle between \mathbf{k} and \mathbf{q} . Graphene conductivity can then be calculated by the Boltzmann transport theory with $\sigma = (e^2/h)2\tau(\varepsilon_F)vk_F$. The properties of graphene's Dirac fermions depends on the dimensionless coupling constant $\alpha_{gr} = ge^2/v\epsilon\hbar$.

B. RPA ground state energy in a gapped graphene

The ground-state energies is calculated by using the coupling constant integration technique, which has the contributions $E_{tot} = E_{kin} + E_x + E_c$. The kinetic energy per particle is easily calculated as $2\varepsilon_F[(1 + \Delta^2/\varepsilon_F^2)^{3/2} - \Delta^3/\varepsilon_F^3]/3$.

The first-order, exchange contribution per particle is given by

$$\varepsilon_x = \frac{E_x}{N} = \frac{1}{2} \int \frac{d^2\mathbf{q}}{(2\pi)^2} v_q \left[-\frac{1}{\pi n} \int_0^{+\infty} d\Omega \chi^{(0)}(\mathbf{q}, i\omega, \mu) - 1 \right]. \quad (12)$$

To evaluate the correlation energy in the RPA, we follow a standard strategy for uniform continuum models²⁸

$$\varepsilon_c^{\text{RPA}} = \frac{E_c}{N} = \frac{1}{2\pi n} \int \frac{d^2\mathbf{q}}{(2\pi)^2} \int_0^{+\infty} d\omega \left\{ v_q \chi^{(0)}(\mathbf{q}, i\omega, \mu) + \ln \left[1 - v_q \chi^{(0)}(\mathbf{q}, i\omega, \mu) \right] \right\}. \quad (13)$$

Since $\chi^{(0)}(\mathbf{q}, i\omega, \mu)$ is linearly proportional to \mathbf{q} at large \mathbf{q} and decrease only like ω^{-1} at large ω in both gapped and gapless graphene, accordingly the exchange and correlation energy built by Eqs. (12) and (13) are divergent.^{19,21} In order to improve convergence, it is convenient at this point to add and subtract vacuum polarization, $\chi^{(0)}(\mathbf{q}, i\omega, \mu = \Delta)$, inside the frequency integral and regularize the exchange and correlation energy. Therefore, these ultraviolet divergences can be cured calculating

$$\delta\varepsilon_x = -\frac{1}{2\pi n} \int \frac{d^2\mathbf{q}}{(2\pi)^2} v_q \int_0^{+\infty} d\omega \delta\chi^{(0)}(\mathbf{q}, i\omega, \mu) \quad (14)$$

and

$$\delta\varepsilon_c^{\text{RPA}} = \frac{1}{2\pi n} \int \frac{d^2\mathbf{q}}{(2\pi)^2} \int_0^{+\infty} d\omega \left\{ v_q \delta\chi^{(0)}(\mathbf{q}, i\omega, \mu) + \ln \left[\frac{1 - v_q \chi^{(0)}(\mathbf{q}, i\omega, \mu)}{1 - v_q \chi^{(0)}(\mathbf{q}, i\omega, \mu = \Delta)} \right] \right\}, \quad (15)$$

where $\delta\chi^{(0)}$ is the difference between the doped ($\mu > \Delta$) and undoped ($\mu = \Delta$) polarization functions. With this regularization, the q integrals have logarithmic ultraviolet divergences.¹⁹ we can introduce an ultraviolet cutoff for the wave vector integrals $k_c = \Lambda k_F$ which is the order of the inverse lattice spacing and Λ is dimensionless quantity. Once the ground-state is obtained the compressibility κ can easily be calculated from $\kappa^{-1} = n^2 \frac{\partial^2 (n\delta\varepsilon_{\text{tot}})}{\partial n^2}$, where the total ground-state energy per particle is given by $\delta\varepsilon_{\text{tot}} = \delta\varepsilon_{\text{kin}} + \delta\varepsilon_x + \delta\varepsilon_c^{\text{RPA}}$. The compressibility of noninteracting gapless graphene is $\kappa_0^0 = 2/(n\varepsilon_F)$ and the compressibility of noninteracting gapped graphene is given by $\kappa_0 = 2/n\varepsilon_F(1 + \Delta^2/\varepsilon_F^2)^{1/2}$.

III. NUMERICAL RESULTS

In this section, we present our calculations for the ground-state properties of gapped graphene in a continuum model at low energy, using the model described in the previous section. Our results are considered a n-doped graphene sheet with $\alpha_{\text{gr}} = 1$ and 2 where it is a typical value thought to apply to graphene sheets on the surface of a SiC or boron nitride substrates. We expect that the physics of gapped graphene is different from gapless graphene due to the sublattice symmetry breaking. In the follow, we will investigate these differences, quantitatively.

Fig. 1 shows the noninteracting dynamic polarization function, $\chi^{(0)}(\mathbf{q}, i\omega, \mu)$ of both gapped and gapless graphene in units of the noninteracting density of state at the Fermi surface, $D(\varepsilon_F)$ as functions of q/k_F and ω/ε_F . In both cases, $\chi^{(0)}(\mathbf{q}, i\omega, \mu)$ linearly diverges with q at small wavelength region and decays as $1/\omega$ at large frequency for finite Δ values due to interband fluctuations in contrast to the ordinary 2D electron gas.

The function $-\chi^{(0)}(\mathbf{q}, 0, \mu)$ contains a number of noteworthy features is shown in Fig. 2(a). First, as we mentioned before, the $q \rightarrow 0$ limit of the static polarization function is a measure of the number of excited states. Second, the derivative of $\chi^{(0)}(\mathbf{q}, 0, \mu)$ at $q = 2k_F$ is singular at finite Δ values the same as the normal 2D electron gas. Note that

$\chi^{(0)}(\mathbf{q}, 0, \mu)$ at $\Delta = 0$ is a smooth function. We stress here that the second order correction of the noninteracting polarization function is mostly responsible to this behavior. This singular behavior is responsible for several interesting phenomena such as Friedel oscillations and the associated RKKY interaction.²⁸ Interestingly, $\chi^{(0)}(\mathbf{q}, 0, \mu)$ reduces to the conventional 2D noninteracting dynamic polarization function at very large Δ values. In this figure, we have shown $-\chi^{(0)}(\mathbf{q}, 0, \mu)$ at $\Delta = 10\varepsilon_F$ which is exactly the same as the conventional 2D noninteracting dynamic polarization function up to mid q values. The behavior of $\chi^{(0)}(\mathbf{k}_F, i\omega, \mu)$ in unit of the density of state of gapped graphene for various Δ is displayed in Fig. 2(b).

As an application of the noninteracting polarization function given by Eq. (6), we calculate the electric conductivity using the Boltzmann equation. we assume $d = 1\text{\AA}$ and $\alpha_{gr} = 2$. Band gap and density dependence of d.c. conductivity are shown in Fig. 3. Increasing disorder (increasing n_i or decreasing d for charge-disorder potential) decrease the σ however increasing the gapped value decreases the d.c. conductivity. Our calculations show that σ decreases by increasing Δ as a function of n/n_i . Moreover, the density dependence of σ is linear at small d and Δ values and deviates from linearity at large d values.²⁹ In the inset, we have shown the results for $d = 10\text{\AA}$ which physically determine that the value of σ increases by increasing d . Interestingly, a large value of σ will be obtained for suspended graphene or by using the SiO_2 substrate instead of using boron nitride or SiC which result in the opening a gap due to symmetry breaking between sublattices.

We also calculated the exchange and correlation energies as a function of Δ for various values of the cutoff Λ . The results are summarized in Fig. 4. we have found that the band gap effects become more appreciable at large cutoff values. The exchange energy is positive¹⁹ because our regularization procedure implicitly selects the chemical potential of undoped graphene as the half gap energy; doping either occupies quasiparticle states with energies larger than Δ , or empties quasiparticles with energies smaller than $-\Delta$. Figure 4(b) shows the correlation energy $\delta\varepsilon_c$ as a function of Δ . Note that $\delta\varepsilon_c$ has the same density dependence as $\delta\varepsilon_x$ apart from the weak dependence on Δ . In contrast to the exchange energy, Figure 4(a), the correlation energy is negative¹⁹. It is important to note that there is a similar behavior between the kinetic energy and the exchange-correlation energy as a function of Δ . The kinetic energy is a slowly varying function to Δ at small gap values and increases by increasing Δ in middle and large values. Consequently, the total energy increases as a function of Δ . Fig. 5 is shown the total ground-state energy. In the inset, the total energy per particle is shown as a function of Δ for various values α_{gr} at $\Lambda = 50$.

Figure 6 shows the charge compressibility, κ/κ_0^0 scaled by its noninteracting gapless compressibility as a function of Δ for different Λ values. The behavior of κ suggests some novel physics qualitatively different from the physics known in the conventional 2D electron gas.^{19,21} Kinetic energy and the exchange-correlation energy make negative contributions to the compressibility and therefore reduces the compressibility by increasing the Δ .

IV. CONCLUSION

We have studied the ground-state thermodynamic properties of a gapped graphene sheet within the random phase approximation (RPA). Note that for a doped graphene the Fermi liquid description is valid. Our aim in this paper is investigating the ground-state properties of a gapped graphene sheet by going from a system with a linear dispersion relation with vanishing the energy gap, $\Delta = 0$ to a system with a parabolic dispersion relation where $\Delta \rightarrow \infty$. To achieve this goal, we have calculated the band gap dependence of noninteracting dynamic polarization function for doped graphene sheet. As a consequence, We have presented results for the conductivity suppression over a wide range of energy gap. We have presented results of ground-state energies by incorporating many-body electron-electron interactions via RPA for gapped graphene sheet. The total ground-state energy increases by increasing the band gap values. This manner occurs based on our model Hamiltonian. We have finally presented results for the charge compressibility suppression over the energy gap. Importantly, the impact of gap energy on the thermodynamic properties would be noticeable for $\Delta \geq 0.2\varepsilon_F$.

Our results demonstrate the importance of including correlation effects together with the gap effects in the thermodynamic quantities of a gapped graphene. It should be possible to extend our work to include disorder effects. Another direction would be to consider the effects of temperature in the thermodynamic quantities.

Acknowledgments

We would like to thank M. M. Vazifeh and Kh. Hassani for helpful discussions. A. Q. is supported by IPM grant.

-
- ¹ K. S. Novoselov, A. K. Geim, S. V. Morozov, D. Jiang, Y. Zhang, S. V. Dubonos, I. V. Grigorieva, and A. A. Firsov, *Science* **306**, 666 (2004); K. S. Novoselov, D. Jiang, F. Schedin, T. J. Booth, V. V. Khotkevich, S. V. Morozov and A. K. Geim, *Prog. Natl. Acad. Soc. USA* **102**, 10451 (2005); Y. Zhang, Joshua P. Small, Michael E. S. Amori and Philip Kim, *Phys. Rev. Lett.* **94**, 176803 (2005) .
- ² A. K. Geim and K. S. Novoselov, *Nature Mater.* **6**, 183 (2007) ; A. K. Geim and A. H. MacDonald, *Phys. Today* **60**, 35 (2007); A. H. Castro Neto, F. Guinea, N. M. Peres, K. S. Novoselov and A. K. Geim, *cond-mat/0709.1163* .,
- ³ S. V. Morozov, K. S. Novoselov, M. I. Katsnelson, F. Schedin, D. C. Elias, J. A. Jaszczak, and A. K. Geim, *Phys. Rev. Lett.* **100**, 016602 (2008); Xu Du, Ivan Skachko, Anthony Barker, Eva Y. Andrei, *Nature Nanotechnology* **3**, 491 (2008); K. I. Bolotin, K. J. Sikes, Z. Jiang, M. Klima, G. Fudenberg, J. Hone, P. Kim, H. L. Stormer, *Solid State Commun.* **146**, 351 (2008) .
- ⁴ C. R. Dean, B. A. Piot, P. Hayden, S. Das sarma, G. Gervais, L. N. Pfeiffer and K. W. West, *Phys. Rev. Lett.* **100**, 146803 (2008) .
- ⁵ Y. W. Son, M. L. Cohen and S. G. Louise, *Phys. Rev. Lett.* **97**, 216803 (2006); M. Y. Han, B. Ozyilmaz, Y. Zhang and P. Kim, *ibid* **98**, 206805 (2007) .
- ⁶ D. A. Abanin, P. A. Lee, L. S. Levitov, *Phys. Rev. Lett.* **96**, 176801 (2006); Y.-W. Son, M. L. Cohen and S. G. Louie, *Nature* **444**, 347 (2006) .
- ⁷ Taisuke Ohta, Aaron Bostwick, Thomas Seyller, Karsten Horn, and Eli Rotenberg, *Science* **313**, 951(2006) .
- ⁸ I. Zanella, S. Guerini, S. B. Fagan, J. Mendes Filho and A. G. Souza Filho. *Phy. Rev. B* **77**, 073404 (2008) .
- ⁹ Francois Varchon , R. Feng , J. Hass, X. Li, Bich N. Nguyen, Ccile Naud, Pierre Mallet, Jean Yves Veuillen , Claire Berger, E. H. Conrad, Laurence Magaud, *Phys. Rev. Lett.* **99**, 126805 (2007); D. S. L. Abergel, A. Russell, Vladimir I. Fal'ko, *Applied Physics Letters* **91**, 063125 (2007); S.Y. Zhou, G.-H. Gweon, A.V. Fedorov, P.N. First, W.A. de Heer, D.-H. Lee, F. Guinea, A.H. Castro Neto, A. Lanzara, *Nature Materials* **6**, 770 (2007); Jakub Kedzierski, Pei-Lan Hsu, Paul Healey, Peter Wyatt, Craig Keast, Mike Sprinkle, Claire Berger, Walt de Heer, *arXiv: IEEE* **55**, 2078 (2008) .

- ¹⁰ Gianluca Giovannetti, Pet A. Khomyako, Geert Brocks, Paul J. Kelly and Jeeroen Van den Brink, Phys. Rev. B **76**, 073103 (2007) .
- ¹¹ V. P. Gusynin, S. G. Sharapov and J. P. Carbotte, Int. J. M. Phys. B**21**, 4611 (2007) and references therein .
- ¹² R. M. Ribeiro, N. M. R. Peres, J. Coutinho and P. R. Briddon, Phys. Rev. B **78**, 075442 (2008); Eduardo V. Castro, K. S. Novoselov, S. V. Morozov, N. M. R. Peres, J. M. B. Lopes dos Santos, Johan Nilsson, F. Guinea, A. K. Geim and A. H. Castro Neto, Phys. Rev. Lett. **99**, 216802 (2007) .
- ¹³ Chang-Yu Hou, Claudio Chamon and Christopher Mudry, Phys. Rev. Lett.**98**, 186809 (2007) .
- ¹⁴ Yugui Yao, Xiao-Liang Qi, Shou-Cheng Zhang and Zhang Fang, Phys. Rev. B**75**, 041401(R) (2007); C. L. Kane and E. J. Mele, Phys. Rev. Lett.**95**, 226801 (2005); Hongki Min, J. E. Hill, N. A. Sinitsyn, B. R. Sahu, Leonard Kleinman and A. H. MacDonald, Phys. Rev. B**74**, 165310 (2006) .
- ¹⁵ S. Murakami, N. Nagaos and S.-C. Zhang, Phys. Rev. Lett.**93**, 156804 (2004) .
- ¹⁶ J. Martin, N. Akerman, G. Ulbricht, T. Lohmann, J. H. Smet, K. von Klitzing, and A. Yacoby, Nature Physics**4**, 144 (2008) .
- ¹⁷ N.M.R. Peres, F. Guinea, and A.H. Castro Neto, Phys. Rev. B **72**, 174406 (2005) .
- ¹⁸ E.H. Hwang, B.Y.-K. Hu, and S. Das Sarma, Phys. Rev. Lett. **99**, 226801 (2007).
- ¹⁹ Y. Barlas, T. Pereg-Barnea, M. Polini, R. Asgari and A. H. MacDonald, Phys. Rev. Lett. **98**, 236601 (2007) .
- ²⁰ D.E. Sheehy and J. Schmalian, Phys. Rev. Lett. **99**, 226803 (2007) .
- ²¹ R. Asgari M. M. Vazifeh, M. R. Ramezanali, E. Davoudi and Tanatar, Phys. Rev. B **77**, 125432 (2008) .
- ²² E.H. Hwang, and S. Das Sarma, Phys. Rev. B**75**, 205418 (2007) .
- ²³ K.W.-K. Shung, Phys. Rev. B, **34**, 979 (1986); J. González, F. Guinea, and M.A.H. Vozmediano, Nucl. Phys. B**424**, 595 (1994); B. Wunsch, T. Stauber, F. Sols, and F. Guinea, New J. Phys. **8**, 318 (2006); X.-F. Wang and T. Chakraborty, Phys. Rev. B **75**, 041404 (2007) .
- ²⁴ Valeri N. Kotov, Vitor M. Pereira, Bruno Uchoa, Physical Review B **78**, 075433 (2008) .
- ²⁵ S. A. Chin, Ann. Phys. **108**, 301 (1977) .
- ²⁶ S. Adam, E.H. Hwang, and S. Das Sarma, Physica E **40**, 1022 (2008); S. Adam, E.H. Hwang, V.H. Galitski, and S. Das Sarma, Proc. Natl. Acad. Sci. **104**, 18392 (2007) .
- ²⁷ D. Novikov, Appl. Phys. Lett. **91**, 102102 (2007); Phys. Rev. B**76**, 245435 (2007) .
- ²⁸ G.F. Giuliani and G. Vignale, *Quantum Theory of the Electron Liquid* (Cambridge University Press, Cambridge, 2005) .
- ²⁹ E.H. Hwang, S. Adam, and S. Das Sarma, Phys. Rev. Lett. **98**, 186806 (2007) .

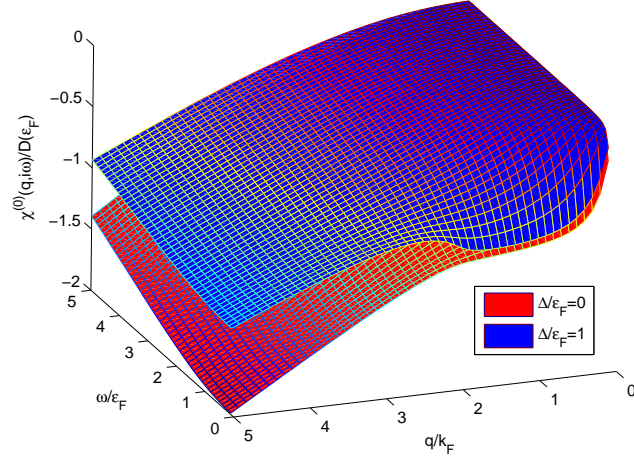


FIG. 1: (Color online) Noninteracting dynamic polarization function for both gapped and gapless graphene in units of density of state, $D(\epsilon_F)$ as functions of q/k_F and ω/ϵ_F .

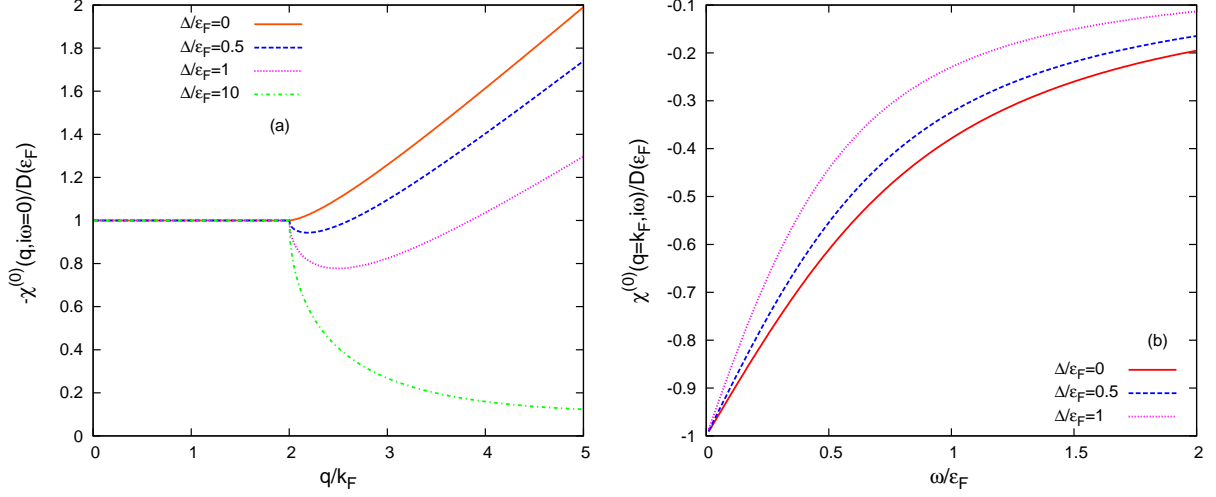


FIG. 2: (Color online) (a): Static noninteracting polarization function as a function of q/k_F for various Δ . (b): $\chi^{(0)}(q = k_F, i\omega, \mu)$ as a function of ω/ϵ_F for various Δ .

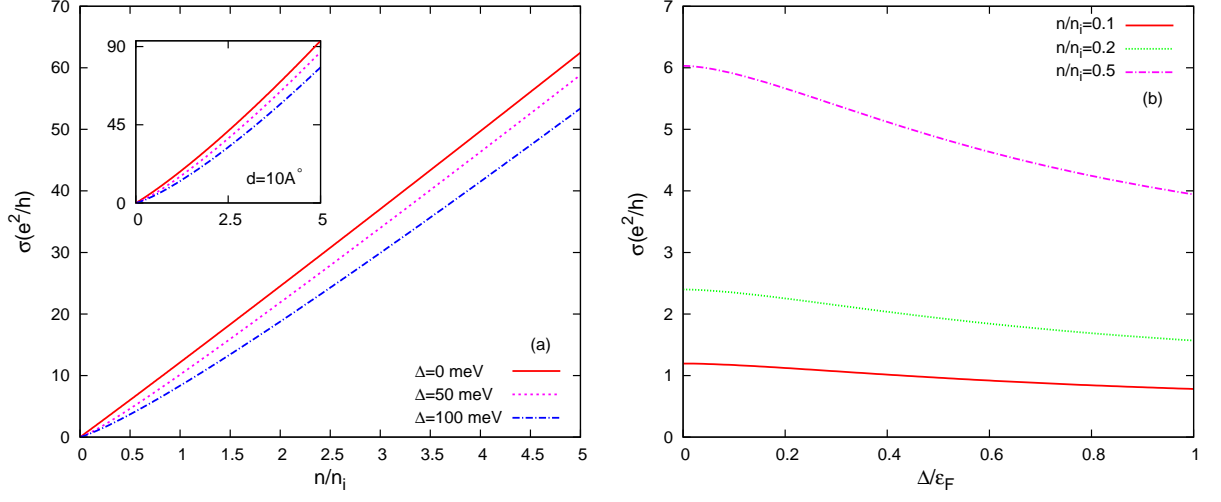


FIG. 3: (Color online) (a): Conductivity as a function of n/n_i for several energy gaps at $d = 1 \text{ \AA}$, in the inset at $d = 10 \text{ \AA}$ (b): Conductivity as a function of Δ for various electron densities per impurity density.

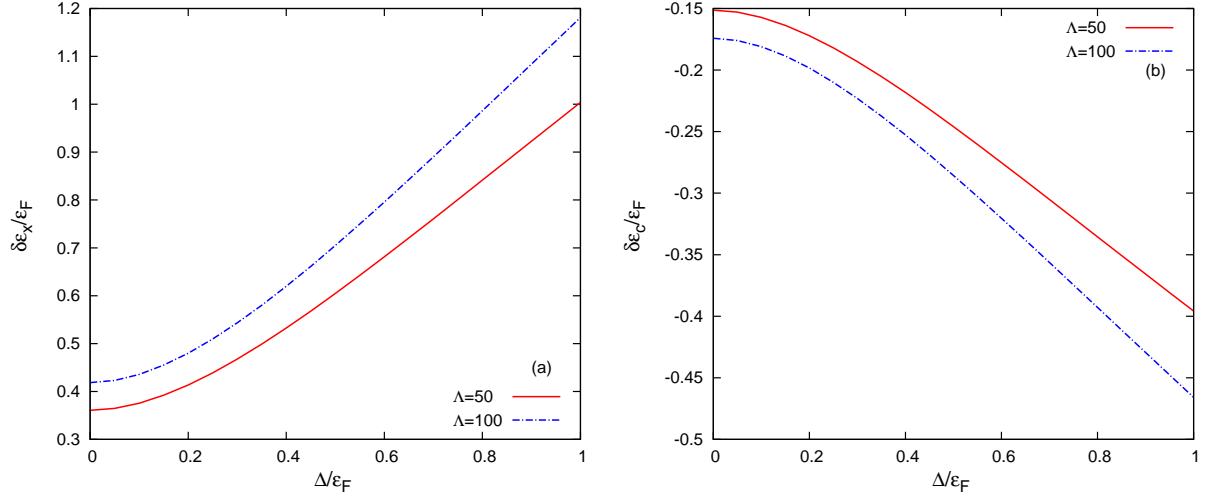


FIG. 4: (Color online) Exchange (a) and correlation (b) energies as a function of Δ for various cutoff Λ at $\alpha_{gr} = 2$.

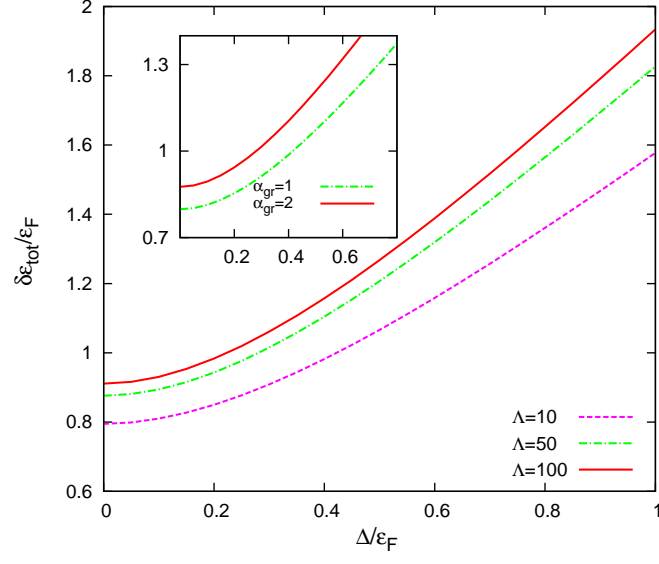


FIG. 5: (Color online) Total ground-state energy per particle as a function of gap energy, Δ for various values of the cutoff Λ at $\alpha_{gr} = 2$. In the inset the total ground-state energy per particle is shown as a function of Δ for various values of α_{gr} at $\Lambda = 50$.

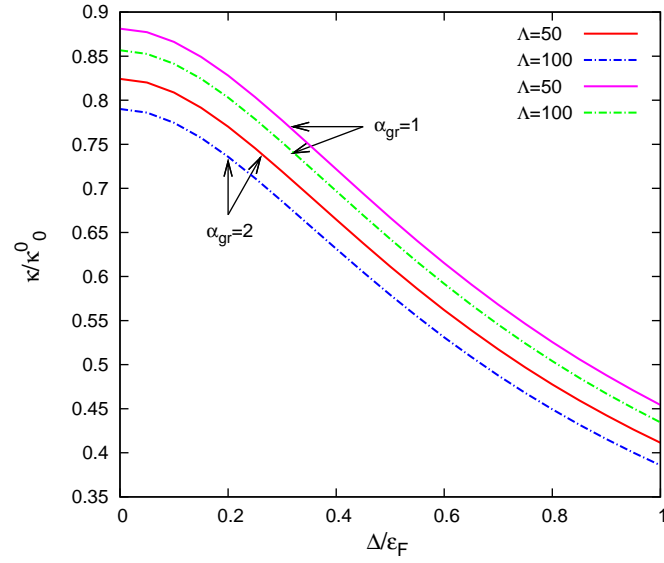


FIG. 6: (Color online) Compressibility κ/κ_0^0 scaled by that of a noninteracting gapless system as a function of Δ for various α_{gr} and Λ .